Integrated Geophysical Characterization Of A NAPL−Contaminated Site Using Borehole And Laboratory Measurements

T22B−1142

Jonathan B. Ajo−Franklin * (Stanford)
Jil T. Geller (LBNL)
Ernest L. Majer (LBNL)
John E. Peterson (LBNL)
Kenneth H. Williams (LBNL)
Jerry M. Harris (Stanford)

A Stanford/LBNL Collaboration

1. Introduction

We present preliminary results from an on−going geophysical investigation at the former DOE Pinellas site, a site with confirmed NAPL contamination. The goal of this work was to demonstrate the combined use of high −resolution crosswell seismic and radar datasets for characterization of NAPL distribution in near−surface environments. Although direct geophysical evidence of the presence of NAPLs has not yet been obtained a significant seismic attenuation anomaly observed at the site may be caused by biogenic gas production linked to in−situ degradation of contaminants. With the benefit of continuing core−scale laboratory measurements and further work on integration of our seismic, radar, and logging data we hope to better constrain the source of the observed seismic attenuation and possibly delineate a region with existing residual NAPLs for further study.

2. Site History

The site of our ongoing investigation is a former DOE manufacturing facility located in Pinellas County, Florida (see [M1]). From 1956 to 1994 the Pinellas DOE Plant manufactured neutron generators and other nuclear weapon components. Several solvents used in the fabrication process, including TCE and toluene, were disposed of in an on−site drum dump located on the northeast corner of the property (see [M2],[M3]). Subsequent water quality investigations detected several significant contaminant plumes at the NE site. NAPLs extracted from ground water monitoring wells suggested the presence of significant quantities of free−phase materials in the subsurface, a hypothesis reinforced by the large volume of VOCs recovered as part of a later auger steam−stripping remediation pilot project.

3. Field Acqusition

The core data sets acquired for geophysical site characterization consisted of a curtain of crosswell seismic and radar section extending from a zone of known DNAPL contamination (ROI 1) to a region confirmed as clean (ROI 2). Crosswell seismic data was acquired using a 24−channel Geometrics acquisition system, a 24 phone hydrophone string, and a fluid coupled piezoelectric source (see 3a−f). 19 seismic sections were acquired at interwell spacings from 2 to 8 meters : for most sections, usable signal at up to 6.5 khz was recorded.

Crosswell Acquisition Setup — Seismic Source Control And Acquisition System — Closeup : Source Control

Acquiring Data : Human Winch — Downhole Piezo Sources — Radar Acquisition — Pulse−Ekko Borehole Radar System

Crosswell radar datasets were acquired using a Pulse−Ekko 100 Borehole System (Sensors & Software : see 3g−h) and 200 mhz antennas. Radar data could not be acquired in all of the wells used for seismic measurements due to the presence of conductive (steel) casing at some locations. An attempt was made to match geometries for the seismic and radar surveys by using the same source/receiver spacing (1/8 m). In addition to the crosswell measurements a Mount Sopris system was used to acquire gamma and conductivity logs in all of the relevant wells for use in constraining lithology. Several existing CPT (Cone Pentrometry) push−points were also available for lithology comparisons although the lack of site−specific CPT calibration data made analysis more difficult.

4. Preliminary Processing

After data collection, a standard pre−processing sequence was performed including required file format conversion, the addition of geometry information, and the removal of very low S/N traces. A low−cut filter at 15 mhz was required on the radar datasets to eliminate low−frequency noise in the traces collected near the surface. Traveltime picking was performed before any wave form processing (deconvolution etc) to retain phase information in the first arrival. A first round of tomography was performed using a traditional damped ART (Algebraic Reconstruction Technique) and straight rays for both the seismic and radar datasets. A significant region of seismic attenuation was observed over a large region which was correllated with the contaminated zone (See Site−Wide Vp Image).

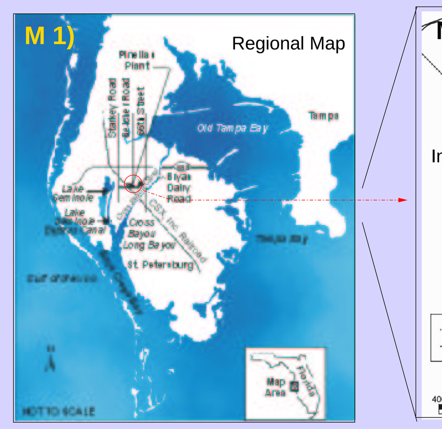

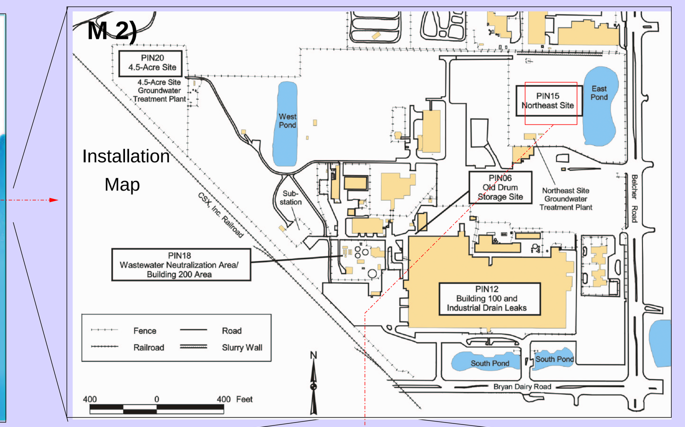

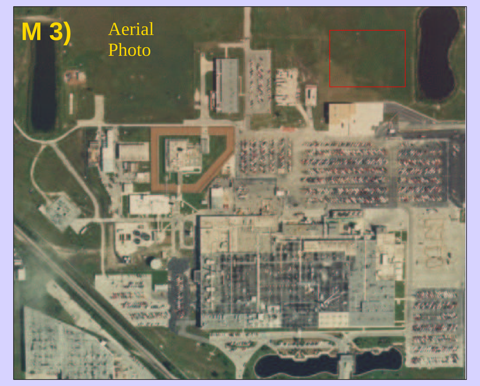

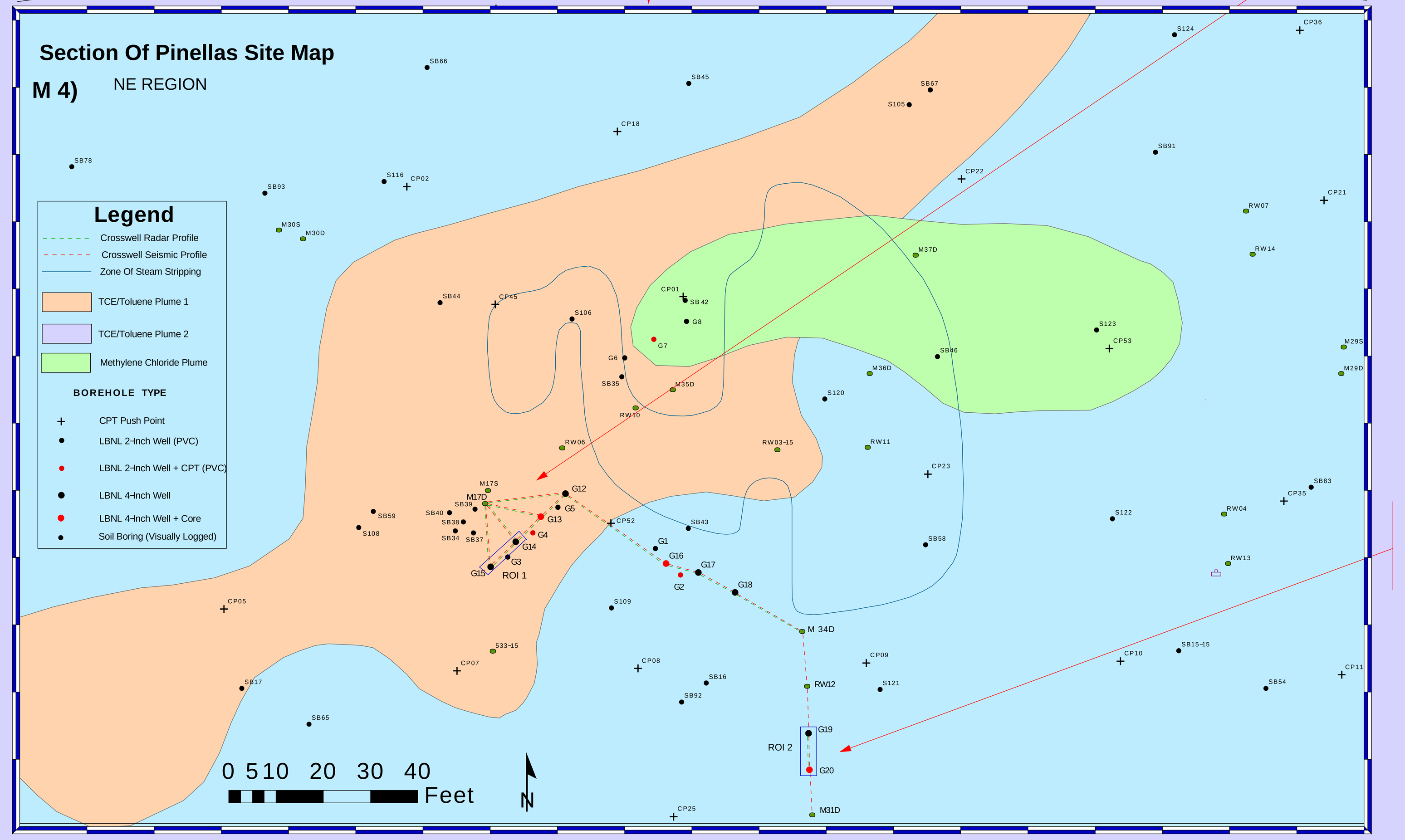

ROI 1 (Dirty Zone) G14−G15

ROI 2 (Clean Zone) G19−G20

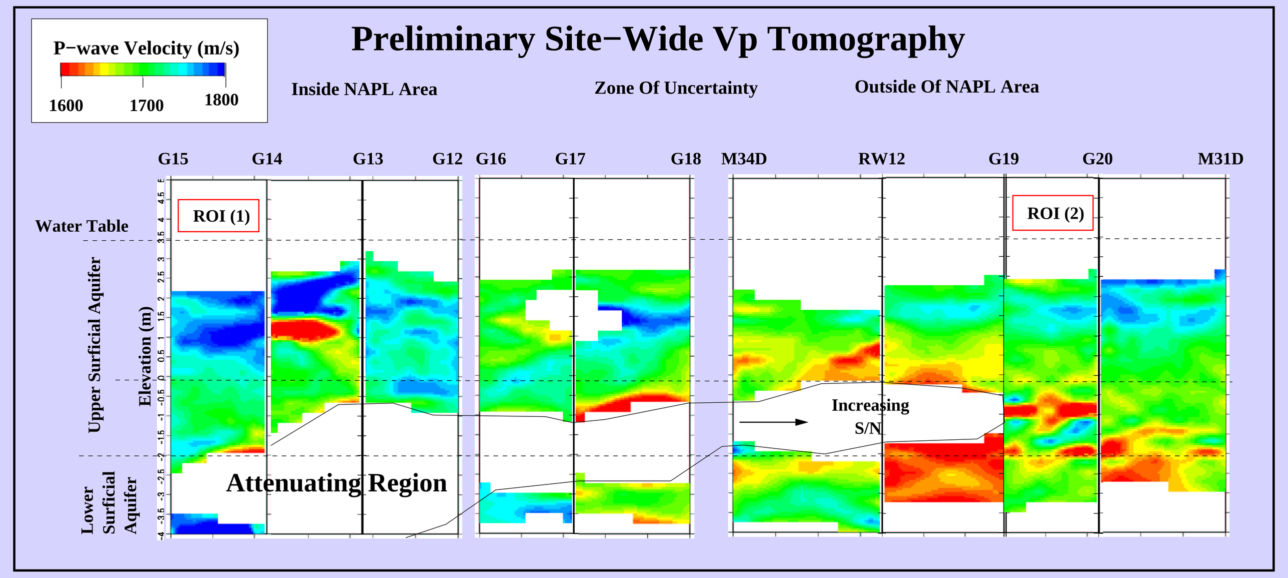

After initial processing of the crosswell datasets two regions were chosen as "regions of interest" (ROI) for full analysis and integration. ROI 1 consisted of well pair G14−G15 within a region of confirmed NAPL contamination while ROI 2 was chosen in a clear zone (well pair G19−G20 − See Site Map). The seismic and radar datasets for each ROI were apertured−matched before traveltime inversion to make the resulting tomograms more consistent. For the integrated processing a slightly more complicated inversion algorithm was used. Initially 1D tomograms were generated using straight rays (thin) and absolute traveltimes with the resulting system solved by GSVD with 2nd order Tikhonov regularization. The 1D regularization parameters were chosen automatically using the Generalized Cross−Validation measure. The 2D tomograms were generated using relative traveltimes with the 1D model used as a prior. Convolution Quelling, a ray broadening technique, was used to insure that the tomograms did not suffer from ray artifacts and to constrain the achievable resolution in the final image. The quelled 2D system was solved using TSVD with the truncation point chosen by observation after the GCV selection technique failed. The observed problems with the GCV algorithm were probably due to the presence of correlated picking errors which break the statistical assumptions underlying cross−validation techniques.

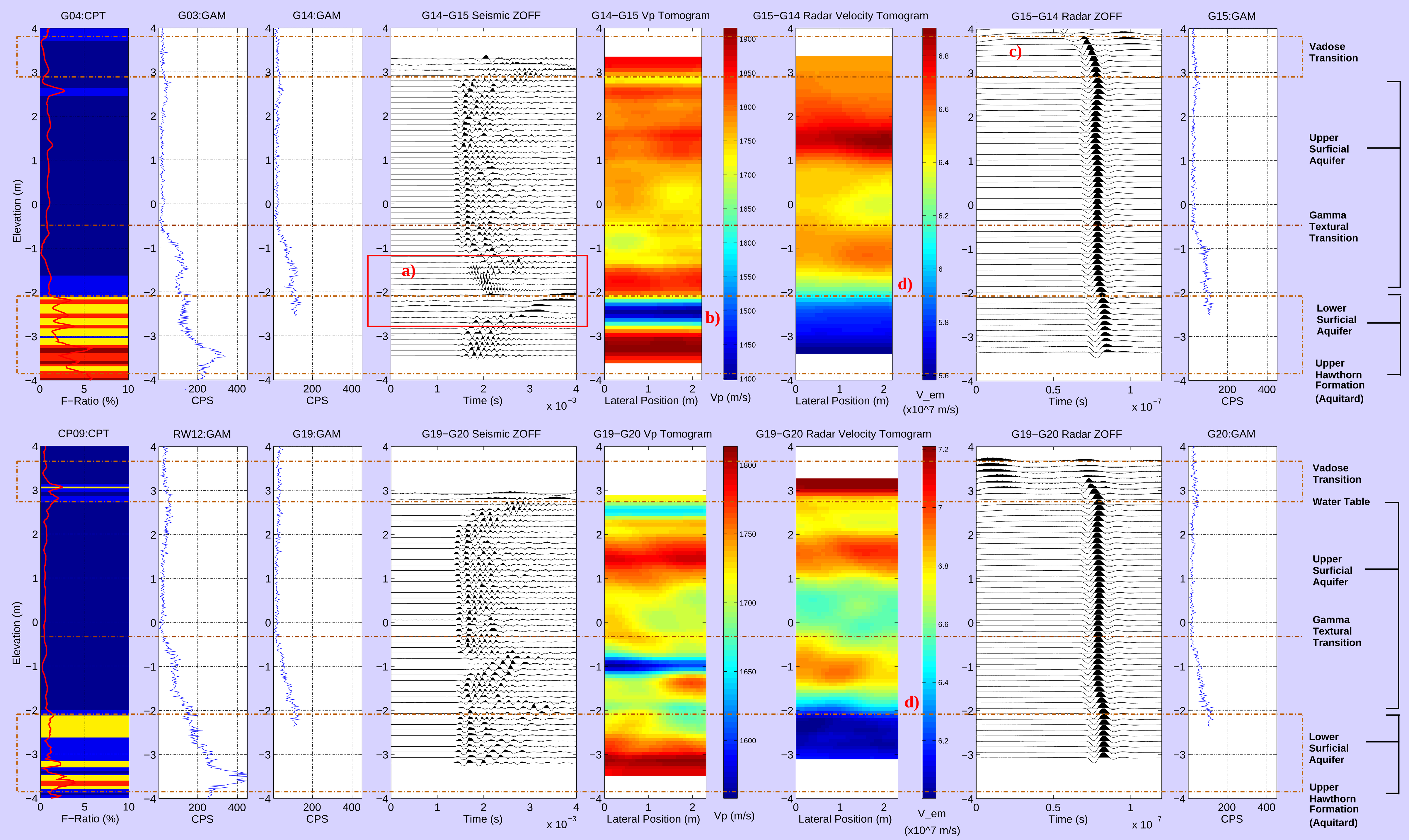

Core−Scale Acoustics Measurements

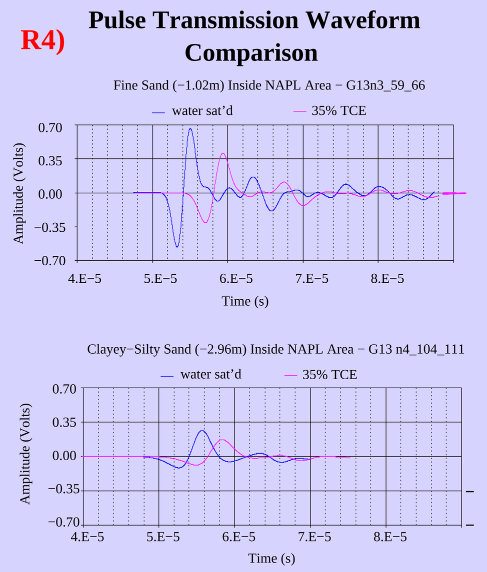

Above : waveform comparison plots for two samples for states of water and partial TCE saturation. Note the velocity and amplitude decrease resulting from TCE saturation. In addition, amplitude differences due to sample texture (fine vs. clayey silt) are visible.

The accuracy of seismic tomogram interpretation in terms of fluid properties is greatly enhanced by core−scale acoustic calibration measurements. To explore the impact of DNAPL saturation on Vp and seismic attenuation we acquired several sections of continous core using a rotary sonic drilling system. After transport back to the laboratory, the cores were drained to increase sample cohesion and scanned using coarse resolution X−Ray CT to identify sections for later examination.

Vp and attenuation measurements were performed on select core sections using a pulse transmission apparatus mounted within a triaxial cell. The samples were intially saturated with water and subsequently injected with either TCE or Toluene, the most relevant contaminants. Figure [R1] compares the physical properties of the two contaminant fluids to air and water. Consistent with our expectations, Vp decreased with TCE and Toluene saturation although the changes are not as significant as previously measured changes in dielectric properties for similar types of contaminant saturated sands.

Observed P−wave amplitudes also decreased with increasing contaminant saturation (R4) but we are not certain that the attenuation effects observed in the field are due to NAPLs or that the mechanism responsible for the core−scale attenuation (~100 khz) are signficant at crosswell frequencies (~5 khz). The basic properties for the samples examined including porosity, texture analysis, and water−saturated Vp are shown in [R2] while Vp and relative amplitude as a function of TCE saturation are plotted in figures [R3] and [R4] for samples within the lower and upper surficial aquifers.

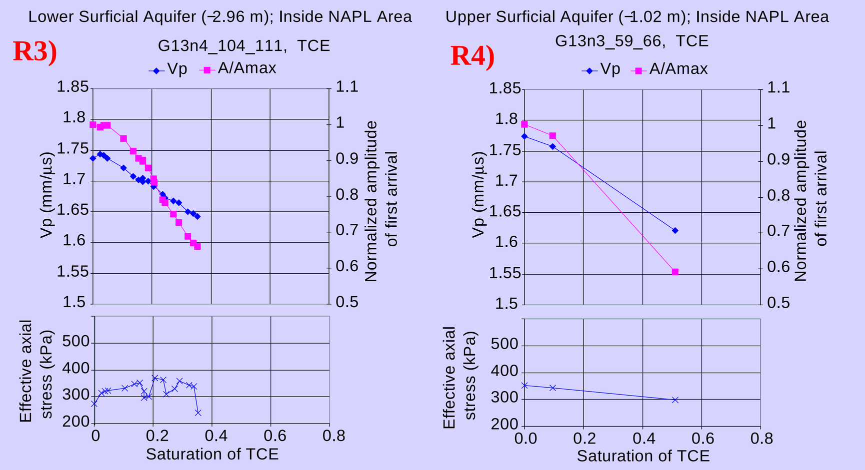

R1) Physical Properties Of Constituent Fluids

Fluid Type	Density ρ (kg/m3)	Acoustic Velocity (Km/s)	Acoustic Impedance ρv (kg/m^2−s)	Bulk Modulus ρv^2 (MPa)	Normal Reflection Coef. (vs. H_2 0)
air	1	0.344	3.44E+02	0.12	+1.0000
water	997	1.497	1.49E+06	2234	−−−−−
toluene	870	1.321	1.15E+06	1518	+0.1300
TCE	1480	1.050	1.55E+06	1632	−0.0202

R2) Core Samples : Basic Measurements

Sample	Elev. (m)	Porosity	Sand/Silt/Clay Fractions	Vp (Water Saturated) (m/s)	NAPL Type	Maximum NAPL Saturation	ΔVp (%)	Δ A (%)
G13n3_59_66	−1.02	0.32	95:1:4	1.77	TCE	0.51	8.62	40.77
G13n4_104_111	−2.96	0.39	67:21:17	1.74	TCE	0.35	5.42	33.93
G13n4_57_64	−2.46	0.39	60:26:14	1.73	Toluene	0.52	5.48	44.07
G20n4_31_38	−2.06	0.36	53:34:13	1.80	Toluene	0.50	8.16	45.67

4. Integrated Analysis

The two panels to the left show the current state of our integrated dataset for ROI 1 and ROI 2 including zero offset waveform plots, radar and seismic velocity tomo−grams, CPT lithology information, and natural gamma logs. The high attenuation region is very distinct on the ROI 1 (G14−G15) seismic ZOFF gather (a). The high attenuation region is also the lowest velocity region in either seismic tomogram : a Vp of aproximately 1400m/s strongly suggests the presence of gas, However the Vp parameters in region (a) are some of the worst resolved variables in the inversion due to the virtual absence of horizontal ray−paths : velocities in that region (b) should be considered carefully.

The top of the Lower Surficial Aquifer was consistently located in the crosswell radar tomograms and matched the CPT derived texture transition region to within 20 cm. The radar surveys also detected a subtle textural tran−−sition at ~ −0.25 m, a region with a gradual increase in fine particle components, which is also visible on the gamma logs. The observed transitions in radar velocity can be largely explained by changes in volumetric water content due to porosity/sorting, or in the case of the lower aquifer boundary, water possibly trapped within the clay component. By the same token the transition between the saturated and unsaturated zone is noticible at the top of the ZOFF gathers as a marked velocity increase although rays which crossed this region were not used in the tomography due to high ray curvature and low S/N levels. More striking than the features visible within the crosswell radar images is the lack of a high velocity zone near the clay boundary which we expected to be the best signature of a zone of high NAPL saturation. The high degree of similarity in the near−clay radar velocities for ROI 1 and ROI 2 suggests that NAPL saturations in contaminated region are below 10%, a level difficult to effectively image using our current approach.

Besides the traditional qualitative data integration methods which only involve consistent processing and comparison of images we are currently exploring several techniques for quantitative integration in both the inversion and interpretation stages. Joint inversions of seismic and radar data which explore a common space of lithological models and rock−physics inversions using multiple geophysical images are just two possibilities.

Disolved Contaminants & Degradation Products

Below : Vinyl chloride is a biologic degradation product and indicates potential for biogenic gas : cis−1,2−DCE is most likely a contaminant as well as a degradation product. Note both the low levels of contaminants and byproduct compunds near G20, one of the ROI 2 wells within the clean zone.

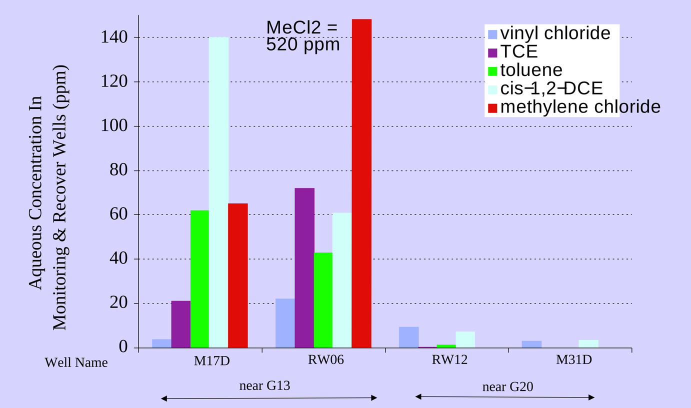

Conclusions And Future Work

We are currently pursuing a more focussed investigation of the observed region of seismic attenuation with the hope of linking Qp to either the presence of contaminants or to biogenic gas production related to NAPLs. Current evidence for a gas related mechanism besides very high levels of seismic attenuation include low P−wave velocities (~ 1400 m/s) and high levels of dissolved vinyl chloride, a gaseous contaminant byproduct, within the dirty region of the site. We are currently processing a hydrophone VSP dataset also collected at the site which may provide additional attenuation information at lower frequencies (~600 hz) to further constrain plausible mechanisms. If we can reliably link the attenuation to NAPL related gas generation than we hope to produce a rough map of likely regions of residual TCE saturation to aid ongoing site remediation efforts.

Acknowledgements

This work was funded by the Subsurface Contamination Focus Area of the Environmental Management Program of USDOE, under contract # DE−AC−03−76F0098. We would also like to thank the EPA for funding the first author through the STAR Fellowship program and the Stanford Department of Geophysics for funding through the Chair's Fellowship For Intergroup Research. This research would not have been possible without the cooperation of the DOE Pinellas Site Staff including Dave Ingle and the MACTEC−ERS Crew. We would also like to thank Cecil Hoffpauier (LBNL), Philip Rizzo (LBNL), and Jaime Urban (Stanford) for assistance in collection field data at Pinellas. Additionally, Liviu Tomutsa was crucial in obtaining the X−Ray CT imagery of our extracted core samples.